Polymer Chemistry

Accepted Manuscript

ROYAL SOCIETY OF CHEMISTRY

www.rsc.org/polymers

Polymer Chemistry

Dynamic Article Links ►

Cite this: DOI: 10.1039/c0xx00000x

www.rsc.org/xxxxxx

ARTICLE

Two-dimensional single-layer supramolecular organic framework that is driven by viologen radical cation dimerization and further promoted by cucurbit[8]uril

Liang Zhang,[a] Tian-You Zhou,[b] Jia Tian,[a] Hui Wang,[a] Dan-Wei Zhang,[a]* Xin Zhao,[b] Yi Liu,[c]* and Zhan-Ting Li[a]*

Received (in XXX, XXX) Xth XXXXXXXXX 20XX, Accepted Xth XXXXXXXXX 20XX
DOI: 10.1039/b000000x

A two-dimensional supramolecular organic framework has been constructed in water from a rigid water-soluble triangular building block which is driven by the dimerization of three appended viologen radical cation units. Cucurbit[8]uril (CB[8]) further stabilizes the single-layer network by encapsulating the stacking viologen radical cation dimers. The new supramolecular networks have been characterized with UV-vis absorption, electron paramagnetic resonance, dynamic light scattering, solution and solid phase small angle X-ray diffraction, and AFM experiments. The aggregation behaviour is in sharp contrast to that of a triangular control compound, which only forms a discrete dimer or 2:3 encapsulation complex in the absence or presence of CB[8].

Introduction

Two-dimensional single-layer networks have attracted great attention in the past decades due to their unique structural feature and potential applications in analytic, sensing, environmental and materials fields.[1] By controlling the polymerization[2] or self-assembly[3] of organic components on solid surfaces, a variety of single-layer soft networks have been constructed. Zuckermann and co-workers have recently reported the assembly of highly ordered 2D nanosheet based on sequence-specific peptoids.[4] Recently, Kim and co-workers reported that single-monomer-thick 2D polymers can be generated in solution through shape-directed covalent linkage of disk-shaped building blocks,[5] and Zhao and co-workers also described the solution-phase preparation of another kind of single-layer 2D polymers from the coupling of triptycene tricatechol with 1,4-benzene- or 4,4'-biphenyldiboronic acids.[6] Such structurally unique 2D soft networks may further serve as useful platforms for addressing new fundamental scientific questions or exploiting new technological applications.[7]

Supramolecular polymerization provides a robust strategy for constructing complicated soft architectures.[8-22] In most cases, simple ditopic monomers are designed to generate linear supramolecular polymers which exhibit discrete properties or functions. Recently, a number of tri-[23-26] and tetratopic building blocks[27-30] have been reported to generate complicated hyper-branched supramolecular polymers or networks.[23-25] It has been established that tritopic arylamide monomers tend to stack in an one-dimensional space to generate column-styled aggregates.[23] Zhang and co-workers described that dialkylated melamine derivatives self-assembled with halogen acids into 2D organic microsheets in organic solvent driven by counter ion-bridged multiple hydrogen bonds.[31] Recently, we reported that a rigid stacking-forbidden 1,3,5-triphenylbenzene compound bearing three 4,4'-bipyridin-1-ium units could be held together by cucurbit[8]uril (CB[8]) in water through hydrophobicity to form a single-layer 2D honeycomb supramolecular organic framework.[32] Herein, we demonstrate that the dimerization of viologen radical cation units appended to a triangular rigid backbone has been utilized to drive the formation of a new 2D supramolecular organic framework in water. We also show that the new ordered self-assembled network can be further stabilized by CB[8] through encapsulating the radical cation dimer.

Results and Discussion

Compound **Tr**$^{6+}\cdot 6Cl^-$ was prepared to exploit its ability of forming 2D ordered networks through the stacking of its viologen units after being reduced to radical cations. Three hydrophilic bis(2-hydroxyethyl)carbamoyl groups were introduced to provide solubility in water and to suppress the stacking of the backbone in the one dimensional space, which is typical of discotic conjugated

---

[a] *Department of Chemistry, Fudan University, 220 Handan Road, Shanghai 200433, China. Fax: +86 21 65641740; Tel: +86 21 65642038; E-mail: zhangdw@fudan.edu.cn; ztli@fudan.edu.cn*
[b] *Shanghai Institute of Organic Chemistry, Chinese Academy of Sciences, 345 Lingling Lu, Shanghai 200032, China*
[c] *The Molecular Foundry, Lawrence Berkeley National Laboratory, Berkeley, CA 94720, USA. E-mail: yliu@lbl.gov*

† Electronic Supplementary Information (ESI) available: details of synthesis and characterizations, additional UV-vis and ESR spectra, DLS, SAXD profile, SEM and AFM images. See DOI: 10.1039/b000000x/

molecules.[33] Compounds $\mathbf{M}^{2+}\cdot 2Cl^-$, $\mathbf{D}^{4+}\cdot 4Cl^-$, and $\mathbf{T}^{6+}\cdot 6Cl^-$ were prepared as controls. All the compounds were soluble in water. Their viologen ($\mathbf{V}^{2+}$) units were readily reduced to radical cation $\mathbf{V}^{\bullet +}$ by sodium dithionite in water.[34] All measurements were performed in sodium phosphate buffer (pH = 7.0) in the presence of a large excess of sodium dithionite to prevent the oxidation of the radical cations.[35]

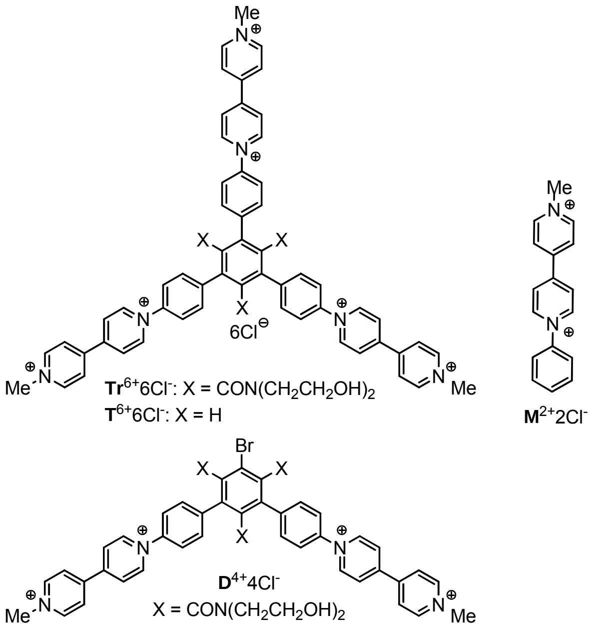

$\mathbf{Tr}^{6+}6Cl^-$: X = $CON(CH_2CH_2OH)_2$

$\mathbf{T}^{6+}6Cl^-$: X = H

$\mathbf{M}^{2+}2Cl^-$

$\mathbf{D}^{4+}4Cl^-$

X = $CON(CH_2CH_2OH)_2$

UV-vis spectra of the four compounds were first recorded in water after their $\mathbf{V}^{2+}$ units were reduced to $\mathbf{V}^{\bullet +}$ radical cation (Fig. 1 and Fig. S1-S10).[29,35] All the spectra displayed two absorption bands (Fig. 1a). A stronger band appeared around 600 nm while the other one, centered around 1000 nm, was relatively weaker and broader, which is typical for the $(\mathbf{V}^{\bullet +})_2$ dimer. The band around 600 nm should be a combination of that of the monomer $\mathbf{V}^{\bullet +}$ and its dimer.[35-37] UV-vis dilution experiments were then performed for all four compounds. By fitting the maximum absorption of dimer $(\mathbf{V}^{\bullet +})_2$ around 1000 nm, where the radical cation $\mathbf{V}^{\bullet +}$ monomer does not produce absorption, to a nonlinear self-binding equation,[29,30] the apparent association constant (K_a) of the dimerization of their $V^{\bullet +}$ units could be determined (Table 1). The K_a value of $\mathbf{M}^{\bullet +}$ was notably higher than that of the radical cation of *N*,*N*'-dialkylated-4,4'-bipyridine,[29] suggesting that the *N*-phenyl substitution enhanced the stacking of the $V^{\bullet +}$ units by extending the conjugated backbone. It can be found that, with the increase of the number of the $\mathbf{V}^{\bullet +}$ units, the apparent K_a increased substantially, which supported that the stacking of the $\mathbf{V}^{\bullet +}$ units of $\mathbf{D}^{2(\bullet +)}$, $\mathbf{T}^{3(\bullet +)}$, and $\mathbf{Tr}^{3(\bullet +)}$ promoted each other. The addition of less polar THF solvent weakened the stacking of the $\mathbf{V}^{\bullet +}$ units of all four compounds, as reflected by the decrease of their apparent K_a values.[29] When the THF volume ratio was increased to 7.5%, no absorption of the dimer $(\mathbf{V}^{\bullet +})_2$ was observed for $\mathbf{M}^{\bullet +}$, and when the content of THF was further increased to 15%, the absorption of the $(\mathbf{V}^{\bullet +})_2$ dimer also vanished from the spectrum of $\mathbf{D}^{2(\bullet +)}$. However, the absorption of the dimer were still preserved in the spectra of $\mathbf{Tr}^{3(\bullet +)}$ and $\mathbf{T}^{3(\bullet +)}$, indicating the relatively high stability of their respective radical cation dimers. In the presence of CB[8], the stability of the $(\mathbf{V}^{\bullet +})_2$ dimer formed by the four compounds were all improved (Fig. 1b), as reflected by the increase of their apparent K_a values (Table 1), which can be reasonably attributed to the encapsulation of the radical cation dimer within CB[8].[35,36] In the presence of CB[8], the apparent K_a value of $\mathbf{Tr}^{3(\bullet +)}$ was still the highest, even though its increase extent was the smallest. This is not unexpected considering the already high stability of its $(\mathbf{V}^{\bullet +})_2$ without the encapsulation of CB[8].

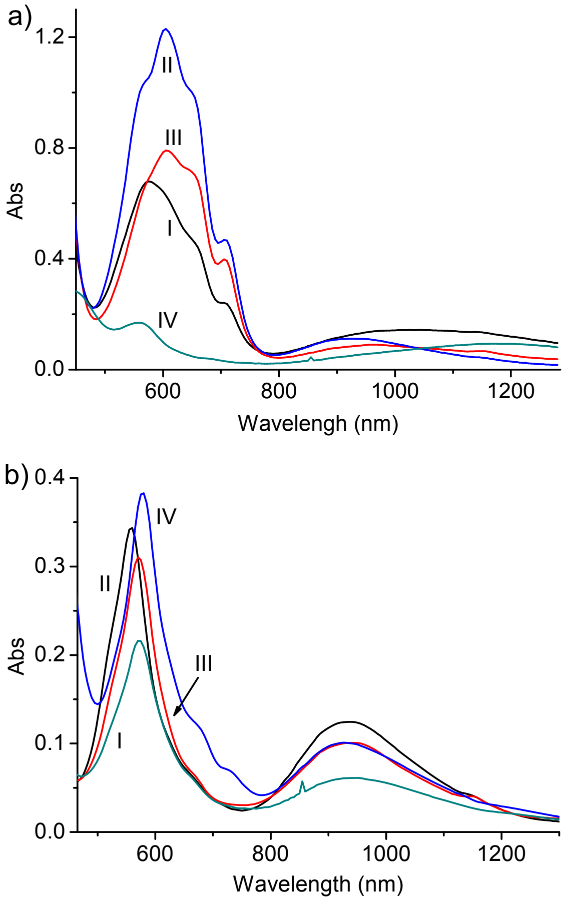

Fig. 1 The absorption spectrum of a) $\mathbf{Tr}^{3(\bullet +)}$ (I, 17 μM), $\mathbf{M}^{\bullet +}$ (II, 50 μM), $\mathbf{D}^{2(\bullet +)}$ (III, 34 μM), and $\mathbf{T}^{3(\bullet +)}$ (IV, 17 μM) in sodium phosphate buffer (0.1 M) containing sodium dithionite (50 mM) at 25 °C and b) of $\mathbf{Tr}^{3(\bullet +)}$ (I, 10 μM), $\mathbf{M}^{\bullet +}$ (II, 30 μM), $\mathbf{D}^{2(\bullet +)}$ (III, 15 μM), $\mathbf{T}^{3(\bullet +)}$ (IV, 10 μM) in sodium phosphate buffer (0.1 M) containing sodium dithionite (50 mM) in the presence of CB[8] (15 μM) at 25 °C.

Table 1 The (apparent) association constants (K_a) of the dimerization of the $\mathbf{V}^{\bullet +}$ unit in sodium phosphate buffer (pH = 7.0)[a]

	H_2O	THF (7.5%)	THF (15%)	H_2O with CB[8][b]
$\mathbf{Tr}^{3(\bullet +)}$	1.2×10^6	8.6×10^5	5.0×10^4	4.5×10^6
$\mathbf{M}^{\bullet +}$	3.5×10^3	-[c]	-[c]	9.6×10^5
$\mathbf{D}^{2(\bullet +)}$	2.5×10^4	9.1×10^2	-[c]	2.0×10^6
$\mathbf{T}^{3(\bullet +)}$	1.4×10^5	3.2×10^4	5.0×10^3	1.0×10^6

[a] In the presence of excess sodium dithionite (0.05 M). [b] [CB[8]] = 0.5 × [$\mathbf{V}^{\bullet +}$]. [c] The absorption of V was too weak to be determined accurately.

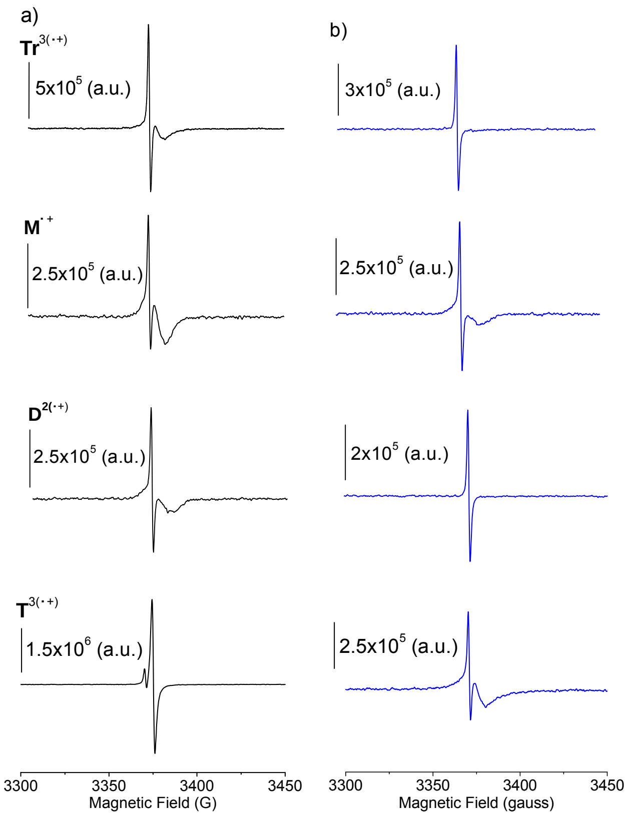

Fig. 2 EPR spectra of $Tr^{3(\bullet+)}$, $M^{\bullet+}$, $D^{2(\bullet+)}$ and $T^{3(\bullet+)}$ ([$V^{\bullet+}$] = 0.1 mM, 25 °C) in sodium phosphate buffer (0.1 M) containing sodium dithionite (50 mM) at 25 °C in the absence a) and presence b) of CB[8] (0.05 mM) b) at 25 °C.

Electron paramagnetic resonance (EPR) spectra of the four radical cation samples were recorded at the identical concentration of the $V^{\bullet+}$ units to gain more insight into their dimerization tendency. The results are shown in Fig. 2. In water, all the spectra showed the existence of a strong, sharp signal and a weak, broad signal. The sharp strong signal is typical for the $(V^{\bullet+})_2$ dimer,[37,38] while the weak broad one should be that of their $V^{\bullet+}$ monomer (Fig. 2a).[29,37] The strength of the broad signals declined in the order of $M^{\bullet+} > D^{2(\bullet+)} > Tr^{3(\bullet+)}$, which corresponded to the decrease of the concentration of the monomeric $V^{\bullet+}$.[29] In the presence of CB[8], the weak broad signal of $D^{2(\bullet+)}$ and $Tr^{3(\bullet+)}$ disappeared (Fig. 2b), supporting that their $V^{\bullet+}$ units almost exclusively underwent dimerization due to the encapsulation of CB[8]. This typical signal of $(V^{\bullet+})_2$ was maintained even at 80 °C for both samples (Fig. S11,S12). In contrast, the signal of $M^{\bullet+}$ still exhibited a small deformation even at 25 °C (Fig. 2b), indicating the existence of a small amount of the monomeric $V^{\bullet+}$. These results are well consistent with the above quantitative absorption experiments, again supporting that the rigid di- and tritopic frameworks promoted the stacking of their $V^{\bullet+}$ units. The EPR spectrum of $T^{3(\bullet+)}$ displayed a small hyperfine signal. In the presence of CB[8], a weak and broad signal was still observed. Given the very high K_a of its $V^{\bullet+}$ unit (Table 1), this signal was not likely from the $V^{\bullet+}$ monomer. We speculate that it might be produced by another radical cation species whose unpaired electron was relocated to the central aromatic moiety, although the exact structure still remains unclear.[39]

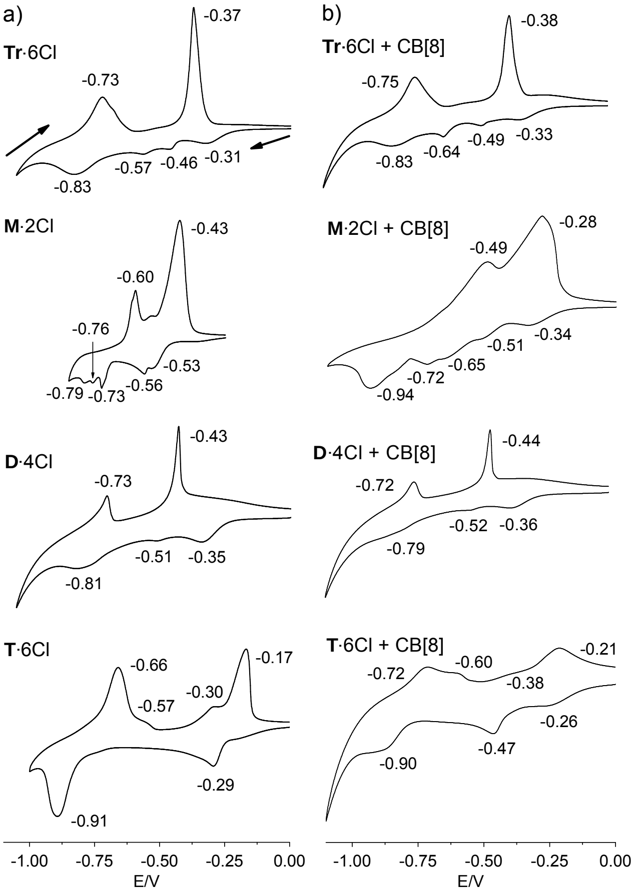

Fig. 3 Cyclic voltammograms of Tr^{6+}·6Cl$^-$, M^{2+}·2Cl$^-$, D^{4+}·4Cl$^-$, and T^{6+}·6Cl$^-$ in aqueous potassium chloride (0.1 M) solution (scan rate: 100 mV/s, [V] = 0.5 mM) in the a) absence and presence of CB[8] ([CB[8]] = 0.5 × [V]).

The electrochemistry of the four compounds was studied by cyclic voltammetry. The obtained cyclic voltammograms (CV) in water were provided in Fig. 3. Compounds M^{2+}·2Cl$^-$, D^{4+}·4Cl$^-$, and Tr^{6+}·6Cl$^-$ exhibited five, three, and four peaks, respectively, on the reductive scan. For M^{2+}·2Cl$^-$, the first two peaks may be attributed to the $M^{2+} \rightarrow M^{\bullet+}$ and $M^{2+} + M^{\bullet+} \rightarrow (M^{\bullet+})_2$ processes, and another three peaks may be produced by the $M^{\bullet+} \rightarrow M$, $(M^{\bullet+})_2 \rightarrow M + M^{\bullet+}$, and $(M^{\bullet+})_2 \rightarrow 2M$ processes. The CV of D^{4+} exhibited three broad reduction waves. The first two should be similar to those of M^{2+}, which led to the formation of $D^{2(\bullet+)}$ and its dimer, while the third broad one might be related to the one-electron reduction of its $V^{\bullet+}$, which existed in different forms, to neutral **V** unit. The CV of Tr^{6+} exhibited four reduction waves. The first three ones were generated through the formation of $V^{\bullet+}$ in different forms, which were difficult to differentiate, and the last one should correspond to the formation of neutral **V** unit from different $V^{\bullet+}$ species. Although all the CVs of the three compounds exhibited multi-step reduction processes, their first reduction potential shifted to the positive direction (from -0.53 of M^{2+} to -0.35 of D^{4+} and to -0.31 V of Tr^{6+}), which supported increasing reduction tendency of their $\mathbf{V}^{2+}$ units due to enhanced dimerization of the resulting $\mathbf{V}^{\bullet+}$. Consistent with this shifting, the last reduction potential, which related to the conversion of $\mathbf{V}^{\bullet+}$ and/or $(\mathbf{V}^{\bullet+})_2$ to neutral **V**, shifted to the more negative direction, This shift indicated the increasing stability of their $(\mathbf{V}^{\bullet+})_2$, the reduction of which required more negative potentials. In the presence of CV[8], the three compounds maintained the same number of reduction waves. However, the first and last reduction potentials of $\mathbf{M}^{2+}$ shifted pronouncedly to the positive and negative direction, pointing to the even increased stability of its $(\mathbf{V}^{\bullet+})_2$ dimer due to the encapsulation of CB[8]. In contrast, such shifts were quite insignificant for $\mathbf{Tr}^{6+}$ and $\mathbf{D}^{4+}$, which were reasonable considering that their $(\mathbf{V}^{\bullet+})_2$ were already highly stable and didn't gain much stabilization from the encapsulation of CB[8].

The CV of $\mathbf{M}^{2+}$, $\mathbf{D}^{4+}$, and $\mathbf{Tr}^{6+}$ all exhibited two oxidation waves (Fig. 3). The respective potential differences were increased from 0.17 to 0.30 to 0.36 V. This tendency remained the same upon addition of CB[8], although the potential differences were changed notably. These observations also supported the increase of the stability of their $(\mathbf{V}^{\bullet+})_2$ with the increase of their **V** units, which caused the formation of the $(\mathbf{V}^{\bullet+})_2$ more easily and the loss of electron from the dimer more difficultly.

The CV of $\mathbf{T}^{6+}$ exhibited two reduction waves. With the addition of CB[8], these two waves shifted slightly with a new peak appearing at -0.47 V, which might be attributed to the formation of a new $\mathbf{V}^{\bullet+}$ species with the unpaired electron being delocalized to the central aromatic moiety.[39,40] Without or with the addition of CB[8], four oxidation waves were observed in the CV of $\mathbf{T}^{6+}$. In both cases, the first and last waves had a large potential difference, which is also a strong indication that its $(\mathbf{V}^{\bullet+})_2$ was highly stable, similar to that of $\mathbf{Tr}^{6+}$. Increasing or decreasing the scan rate (50-200 mV/s) had a minimal effect on the CV waves of all the four samples in the absence or presence of CB[8].

The above experiments all supported that the stacking of the $\mathbf{V}^{\bullet+}$ units of $\mathbf{Tr}^{3(\bullet+)}$ and $\mathbf{T}^{3(\bullet+)}$ took place in a cooperative manner. Previous report established that the column-styled 1D stacking of a rigid triangular molecule (compound **1** in ESI) similar to $\mathbf{Tr}^{3(\bullet+)}$ was suppressed by the three aliphatic chains.[32] It is thus reasonable to propose that the $\mathbf{V}^{\bullet+}$ units stacked intermolecularly in a 2D space. Given the rigidity of the triangular aromatic framework, such stacking should lead to the formation of a honeycomb-like monolayered supramolecular framework. Only in this framework could the stacking of the $\mathbf{V}^{\bullet+}$ units be maximized, which might hold together a number of components to form a large aggregate. To test this, dynamic light scattering (DLS) experiments were carried out for all the four reduced samples and the results were provided in Fig. 4a. The solutions of $\mathbf{M}^{\bullet+}$, $\mathbf{D}^{2(\bullet+)}$, and $\mathbf{T}^{3(\bullet+)}$ contained very small particles as reflected by their hydrodynamic diameter (D_H), which were comparable with the size of their respective backbone. This result supported that these compounds stacked into small aggregates of two or a little more components. Remarkably, the D_H of the aggregates form by $\mathbf{Tr}^{3(\bullet+)}$ was approximately 18 times the size of the single molecular backbone (ca. 2.5 nm). Since the three amide chains could suppress the 1D stacking of this family of rigid triangular frameworks,[32] the large aggregates could only be generated in a 2D space through the formation of a honeycomb-styled supramolecular organic framework (Fig. 5a).

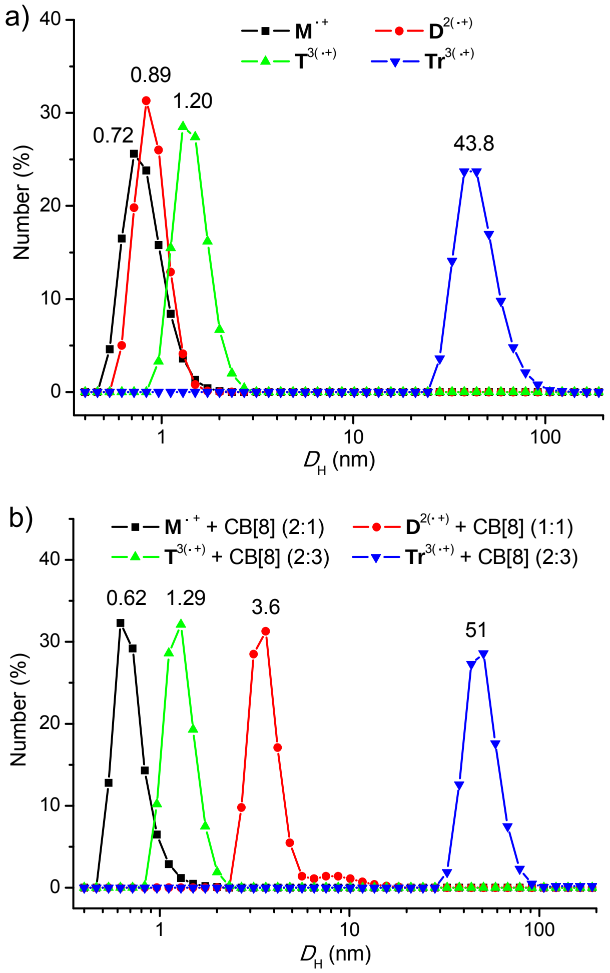

Fig. 4 DLS results of the aqueous solution of $\mathbf{M}^{\bullet+}$, $\mathbf{D}^{2(\bullet+)}$, $\mathbf{T}^{3(\bullet+)}$, and $\mathbf{Tr}^{3(\bullet+)}$, containing sodium dithionite (50 mM), in the a) absence and b) presence of CB[8] ([CB[8]] = 0.14 mM). [**V**] = 0.27 mM).

In the presence of CB[8] of 0.5 molar amount of $\mathbf{V}^{\bullet+}$, the solutions of $\mathbf{M}^{\bullet+}$ and $\mathbf{T}^{3(\bullet+)}$ produced aggregates with the D_H comparable to these without CB[8] (Fig. 4b), implying that in the mixtures the corresponding 2:1 and 2:3 complexes (Fig. 5b) were formed. The D_H for the solution of $\mathbf{D}^{2(\bullet+)}$ notably increased from 0.89 nm to 3.6 nm, which well matched the size of a 6+6 macrocycle which was estimated through molecular dynamics calculation (Fig. 5c). In the presence of CB[8], the large D_H of $\mathbf{Tr}^{3(\bullet+)}$ was further increased pronouncedly, which again supported that this triangular molecule stacked overwhelmingly in a 2D space and the resulting single-layer aggregates were extended due to the "locking" of CB[8] for the $(\mathbf{V}^{\bullet+})_2$ dimers (Fig. 5a). The D_H value determined for the solutions of $\mathbf{Tr}^{3(\bullet+)}$ in the absence and presence of 1.5 equiv of CB[8] were also concentration-dependent (Fig. S13). At the high concentration of 0.17 mM for $\mathbf{Tr}^{3(\bullet+)}$, the values could be increased to 82.5 and 115 nm, respectively.

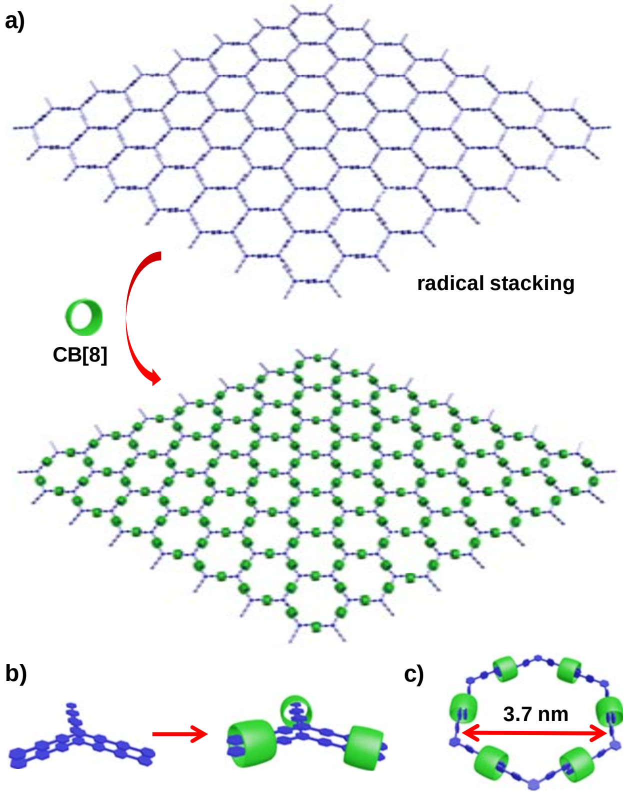

Fig. 5 Schematic presentation of a) the honeycomb-styled 2D supramolecular organic framework formed by $\mathbf{Tr}^{3(\bullet+)}$ and further promoted by CB[8], b) the formation of a 2:3 complex from $\mathbf{T}^{3(\bullet+)}$ and CB[8], c) 6:6 complex of $\mathbf{D}^{2(\bullet+)}$ and CB[8]. Because of the dynamic feature of the stacking interaction, the framework is not perfect and not strictly confined in a plane. Instead, the components might deviate from the plane.

The periodic nature of the layered supramolecular organic framework formed by $\mathbf{Tr}^{3(\bullet+)}$ was further revealed by discrete small angle X-ray diffraction (SAXD) experiments (Fig. 6). The solution phase SAXD profile of the 2:3 mixture of $\mathbf{Tr}^{3(\bullet+)}$ and CB[8] in water, which was obtained with a synchrotron X-ray diffraction facility, revealed a discernible broad diffraction peak with a d spacing of around 3.7 nm (Fig. 6a). A similar diffraction peak was not observed with a common diffraction facility. The value matched well with the expected diameter of the repeating units in the proposed honeycomb supramolecular framework (Fig. 5). The broadening feature of the peak should reasonably reflect the dynamic nature of the 2D supramolecular framework. For the solid sample prepared by reducing $\mathbf{Tr}^{6+}\cdot 6\mathrm{Cl}^-$ with sodium dithionite in water and then evaporating the solvent under a reduced pressure, a broad but apparent peak, corresponding to a d spacing of around 4.3 nm, was observed (Fig. 6b). Molecular dynamics modeling of a hexagonal structure based on six $\mathbf{D}^{2(\bullet+)}$ revealed that, when the two neighboring $\mathbf{V}^{\bullet+}$ units stacked in a face-to-face manner which maximizes π-surface overlapping, the distance between two parallel edges of the hexagon is ca. 3.7 nm (Fig. 5c), and when the stacking occurred only between the peripheral pyridine units, the edge-to-edge distance would increase to ca. 4.5 nm. Thus, for the possible honeycomb 2D supramolecular organic framework formed by $\mathbf{Tr}^{3(\bullet+)}$, an d spacing within the range of 3.7 to 4.5 nm for the neighboring parallel $(\mathbf{V}^{\bullet+})_2$ dimers is expected. The above observed *d* spacing fell into this distance range, thus supporting the formation of the periodic 2D framework. Under the same conditions, the solid sample of the 2:3 mixture of $\mathbf{Tr}^{3(\bullet+)}$ and CB[8] produced a broad diffraction peak which also corresponded to the spacing of 4.3 nm (Fig. S14). When $\mathbf{Tr}^{3(\bullet+)}$ was prepared by reducing $\mathbf{Tr}^{6+}$ with an excess of zinc dust, its solid mixture with CB[8] (2:3) gave rise to a broad, but remarkably stronger diffraction peak corresponding to a d spacing of 4.0 nm (Fig. 6c). All these results pointed to the formation of the periodic honeycomb supramolecular organic framework by $\mathbf{Tr}^{3(\bullet+)}$ in the absence and presence of CB[8].

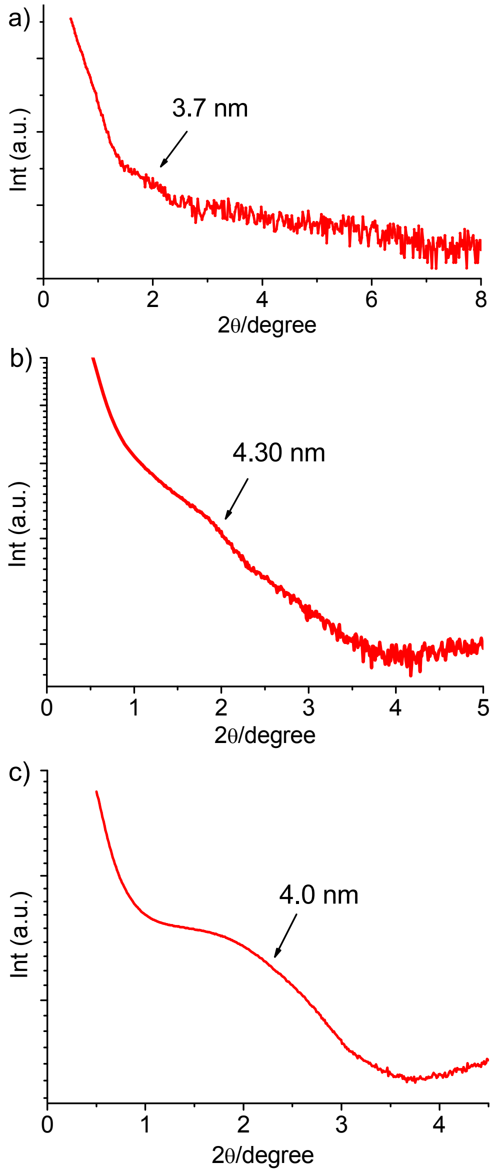

Fig. 6 a) Solution-phase SAXD profile of the mixture of $\mathbf{Tr}^{3(\bullet+)}$ (0.8 mM) and CB[8] (1.2 mM) in water containing sodium dithionite (50 mM). SAXD profile of the solid sample of $\mathbf{Tr}^{3(\bullet+)}$ obtained b) by evaporating the aqueous solution of $\mathbf{Tr}^{6+}\cdot 6\mathrm{Cl}^-$ (1.0 mM) containing sodium dithionite (50 mM) and c) by evaporating the aqueous solution of $\mathbf{Tr}^{6+}\cdot 6\mathrm{Cl}^-$ (1.0 mM) and CB[8] (1.5 mM) after treated with an excess of Zn dust.

The layered structures of the viologen radical cation stacking-based supramolecular systems were further investigated with microscopic techniques. Scanning electron microscope (SEM) images showed that, without or with the addition of CB[8], the samples of $\mathbf{Tr}^{3(\bullet+)}$ all gave rise to thin flakes or films upon drying on mica substrates (Fig. S15-S18). Since the sodium dithionite solution alone only generated flocculent aggregates upon drying (Fig. S19), these thin flakes or films were ascribed to the self-assembled layered structures of $\mathbf{Tr}^{3(\bullet+)}$ or its mixture with CB[8]. Atomic force microscopy (AFM) was also utilized to investigate these self-assembled supramolecular structures. To avoid the interference of sodium dithionite, $\mathbf{Tr}^{3(\bullet+)}$ was generated by treating $\mathbf{Tr}^{6+}$ with an excess of Zn dust. The AFM image of $\mathbf{Tr}^{3(\bullet+)}$ showed that it formed thin aggregates (Fig. S20). However, the height of the aggregates could not be determined. AFM probes were frequently broken during the scanning probably due to that the probe could be easily stuck by the flexible side chains of $\mathbf{Tr}^{3(\bullet+)}$. As expected, the 2:3 mixture of $\mathbf{Tr}^{3(\bullet+)}$ and CB[8] also afforded thin planar aggregates (Fig. 7). Remarkably, these planar aggregates have an average height of 1.74 nm, which matches the thickness of a single-layer network determined by the diameter (1.75 nm) of rigid CB[8]. It is worthy to note that the height was quite uniform for all the measured aggregates (Fig. S21-S24). This result strongly supports the single-layer character of the new 2D supramolecular organic framework (Fig. 5a). AFM images also showed that such single-layer aggregates could not be formed by other three samples.

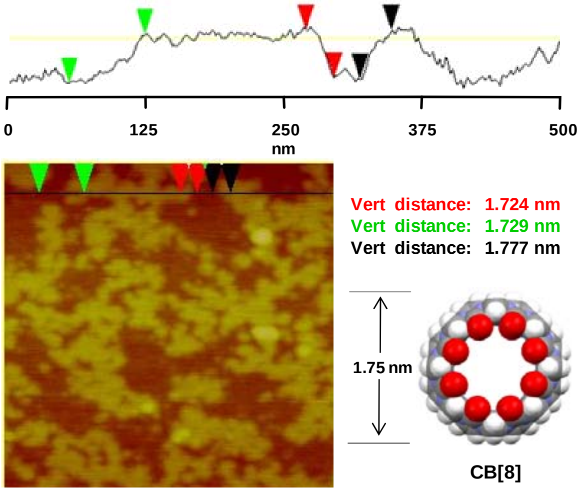

Fig. 7 Tapping-mode AFM image (500 nm × 500 nm) and section analysis of the aggregates on mica from dried solution of compound $\mathbf{Tr}^{6+}\cdot 6Cl^-$ (10 μM) and CB[8] (15 μM) in water after $\mathbf{Tr}^{6+}$ was reduced to $\mathbf{Tr}^{3(\bullet+)}$ with zinc dust. Height analysis versus distance along the black line on the image showed an average thickness of 1.74 nm, consistent with the thickness of the expected monolayer framework, which is equivalent to the diameter of CB[8].

Conclusions

We have demonstrated that single-layer supramolecular organic framework can be generated in water through the self-assembly of a stacking-forbidden triangular monomer in a 2D space driven by strong stacking of the viologen radical cation. This self-assembly itself is highly efficient, and can be further enhanced through the encapsulation of the radical cation dimer with CB[8]. The new supramolecular organic framework and the single-layer feature can be maintained in the solid state, illustrating their high stability. Over years, the dimer of viologen radical cation can be studied only with the assistance of other additional interactions. Our work shows that this dimerizatin pattern can be developed as a robust binding motif for constructing new ordered supramolecular architectures. The formation of 2D self-assembled networks by tri(radical cation) $\mathbf{Tr}^{3(\bullet+)}$ opens the possibility of preparing single-layer polymers in solution by covalent cross-linking of the neighboring molecules.

Acknowledgements

We are grateful to Ministry of Science and Technology (2013CB834501), Ministry of Education (IRT1117), and National Natural Science Foundation (91227108, 21228203, and J1103304) of China, and Science and Technology Commission of Shanghai Municipality (13NM1400200) for financial support and Shanghai Synchrotron Radiation Facility for providing BL14B1 beamline for collecting the solution-phase synchrotron X-ray diffraction data. Y. L. thanks the support from the Molecular Foundry, Lawrence Berkeley National Laboratory, supported by the Office of Science, Office of Basic Energy Sciences, Scientific User Facilities Division, of the U.S. Department of Energy under Contract No. DE-AC02-05CH11231.

Notes and references

1 A. K. Geim, *Science*, 2009, **324**, 1530.

2 L. Grill, M. Dyer, L. Lafferentz, M. Persson, M. V. Peters and S. Hecht, *Nature Nanotech.*, 2007, **2**, 687; L. Lafferentz, V. Eberhardt, C. Dri, C. Africh, G. Comelli, F. Esch, S. Hecht and L. Grill, *Nature Chem.*, 2012, **4**, 215; P. Kissel, R. Erni, W. B. Schweizer, M. D. Rossell, B. T. King, T. Bauer, S. Götzinger, A. D. Schlüter and J. Sakamoto, *Nature Chem.*, 2012, **4**, 28; R. Bhola, P. Payamyar, D. J. Murray, B. Kumar, A. J. Teator, M. U. Schmidt, S. M. Hammer, A. Saha, J. Sakamoto, A. D. Schlüter and B. T. King, *J. Am. Chem. Soc.*, 2013, **135**, 14134.

3 L.-J. Wan, *Acc. Chem. Res.*, 2006, **39**, 334; Y. Yang and C. Wang, *Chem. Soc. Rev.*, 2009, **38**, 2576; K. S. Mali, J. Adisoejoso, E. Ghijsen, I. De Cat and S. De Feyter, *Acc. Chem. Res.*, 2012, **45**, 1309.

4 K. T. Nam, S. A. Shelby, A. B. Marciel, P. C. Choi, T. Chen, L. Tan, T. K. Chu, R. A. Mesch, B.-C. Lee, M. D. Connolly, C. Kisielowski and R. N. Zuckermann, *Nature Mater.*, 2010, **9**, 454; B. Sanii, R. Kudirka, A. Cho, N. Venkateswaran, G. K. Oliver, A. M. Olson, H. Tran, R. M. Harada, T. Tan and R. N. Zuckermann, *J. Am. Chem. Soc.*, 2011, **133**, 20808; G. K. Olivier, A. Cho, B. Sanii, M. D. Connolly, H. Tran and R. N. Zuckermann, *ACS Nano,* 2013, **7**, 9276.

5 K. Baek, G. Yun, Y. Kim, D. Kim, R. Hota, I. Hwang, D. Xu, Y. H. Ko, G. H. Gu, J. H. Suh, C. G. Park, B. J. Sung and K. Kim, *J. Am. Chem. Soc.*, 2013, **135**, 6523.

6 T.-Y. Zhou, F. Lin, Z.-T. Li and X. Zhao, *Macromolecules*, 2013, **46**, 7745.

7 M. S. Spector, E. Naranjo, S. Chiruvolu and J. A. Zasadzinski, *Phys. Rev. Lett.*, 1994, **73**, 2867; J. Sakamoto, J. van Heijst, O. Lukin and A. D. Schlüter, *Angew. Chem. Int. Ed.*, 2009, **48**, 1030; Y. Wang, X. Wang and M. Antonietti, *Angew. Chem., Int. Ed.*, 2012, **51**, 68; L. Chen, Y. Hernandez, X. Feng and K. Müllen, *Angew. Chem. Int. Ed.*, 2012, **51**, 7640.

8 C. Fouquey, J. M. Lehn and A. M. Levelut, *Adv. Mater.*, 1990, **2**, 254; J. M. Lehn, *Polym. Int.*, 2002, **51**, 825.

9 R. P. Sijbesma, F. H. Beijer, L. Brunsveld, B. J. B. Folmer, J. H. K. K. Hirschberg, R. F. M. Lange, J. K. L. Lowe and E. W. Meijer, *Science*, 1997, **278**, 1601; L. Brunsveld, B. J. B. Folmer, E. W. Meijer and R. P. Sijbesma, *Chem. Rev.*, 2001, **101**, 4071; T. F. De

Greef, M. M. J. Smulders, M. Wolffs, A. P. H. J. Schenning, R. P. Sijbesma and E. W. Meijer, *Chem. Rev*., 2009, **109**, 5687.

10 U. S. Schubert and C. Eschbaumer, *Angew. Chem. Int. Ed.*, 2002, **41**, 2892.

11 T. Park, S. C. Zimmerman and S. Nakashima, *J. Am. Chem. Soc.*, 2005, **127**, 6520; T. Park and S. C. Zimmerman, *J. Am. Chem. Soc.*, 2006, **128**, 14236.

12 P. Cordier, F. Tournilhac, C. Soulié-Ziakovic and L. Leibler, *Nature*, 2008, **451**, 977.

13 J. D. Fox and S. J. Rowan, *Macromolecules*, 2009, **42**, 6823.

14 A. Harada, R. Kobayashi, Y. Takashima and A. Hashidzume and H. Yamaguchi, *Nature Chem.*, 2011, **3**, 34.

15 G. Chen and M. Jiang, *Chem. Soc. Rev.*, 2011, **40**, 2254.

16 T. Aida, E. W. Meijer and S. I. Stupp, *Science*, 2012, **335**, 813.

17 E. A. Appel, J. del Barrio, X. J. Loh and O. A. Scherman, *Chem. Soc. Rev.*, 2012, **41**, 6195; D. Das and O. A. Scherman, *Israel J. Chem.*, 2011, **51**, 537.

18 X. Yan, F. Wang, B. Zheng and F. Huang, *Chem. Soc. Rev.*, 2012, **41**, 6042; B. Zheng, F. Wang, S. Dong and F. Huang, *Chem. Soc. Rev.*, 2012, **41**, 1621.

19 S. K. Yang, A. V. Ambade and M. Weck, *Chem. Soc. Rev.*, 2011, **40**, 129.

20 Y. Liu, Z. Huang, X. Tan, Z. Wang and X. Zhang, *Chem. Commun.*, 2013, **49**, 5766; Y. Liu, Z. Wang and X. Zhang, *Chem. Soc. Rev.*, 2012, **41**, 5922.

21 S.-L. Li, T. Xiao, C. Lin and L. Wang, *Chem. Soc. Rev*., 2012, **41**, 5950; T. Xiao, X. Feng, Q. Wang, C. Lin, L. Wang and Y. Pan, *Chem. Commun*., 2013, **49**, 8329.

22 D.-S. Guo and Y. Liu, *Chem. Soc. Rev*., 2012, **41**, 5907; H.-X. Zhao, D.-S. Guo, L.-H. Wang, H. Qian and Y. Liu, *Chem. Commun*., 2012, **48**, 11319.

23 K. Petkau-Milroy, D. A. Uhlenheuer, A. J. H. Spiering, J. A. J. M. Vekemans and L. Brunsveld, *Chem. Sci*., 2013, **4**, 2886; K. Petkau-Milroy, M. H. Sonntag and L. Brunsveld, *Chem. Eur. J*., 2013, **19**, 10786.

24 F. Wang, M. A. J. Illissen, P. J. M. Stals, A. R. A. Palmans and E. W. Meijer, *Chem. Eur. J.*, 2012, **18**, 11761; P. Besenius, G. Portale, P. H. H. Bomans, H. M. Janssen, A. R. A. Palmans and E. W. Meijer, *Proc. Natl. Acad. Sci. U.S.A*., 2010, **107**, 17888.

25 R. Fang, Y. Liu, Z. Wang and X. Zhang, *Polym. Chem*., 2013, **4**, 900.

26 C. Li, K. Han, J. Li, Y. Zhang, W. Chen, Y. Yu and X. Jia, *Chem. Eur. J.*, 2013, **19**, 11892.

27 A. Singh, M. Tolev, M. Meng, K. Klenin, O. Plietzsch, C. I. Schilling, T. Muller, M. Nieger, S. Bräse, W. Wenzel and C. Richert, *Angew. Chem. Int. Ed*., 2011, **50**, 3227.

28 Y. Liu, Z. Huang, K. Liu, H. Kelgtermans, W. Dehaen, Z. Wang and X. Zhang, *Polym. Chem*., 2014, **5**, 53.

29 C. Zhou, J. Tian, J.-L. Wang, D.-W. Zhang, X. Zhao, Y. Liu and Z.-T. Li, *Polym. Chem*., 2014, **5**, 341.

30 J. Tian, Y.-D. Ding, T.-Y. Zhou, K.-D. Zhang, X. Zhao, H. Wang, D.-W. Zhang, Y. Liu and Z.-T. Li, *Chem. Eur. J.*, 2014, **20**, 575.

31 J. Xu, G. Wu, Z. Wang and X. Zhang, *Chem. Sci*., 2012, **3**, 3233; J. Xu, G. Wu, Z. Wang and X. Zhang, *Langmuir*, 2013, **29**, 10959.

32 K.-D. Zhang, J. Tian, D. Hanifi, Y. Zhang, A. C.-H. Sue, T.-Y. Zhou, L. Zhang, X. Zhao, Y. Liu and Z.-T. Li, *J. Am. Chem. Soc*., 2013, **135**, 17913; F. Helmich, C. C. Lee, M. M. L. Nieuwenhuizen, J. C. Gielen, P. C. M. Christianen, A. Larsen, G. Fytas, P. E. L. G. Leclére, A. P. H. J. Schenning and E. W. Meijer, *Angew. Chem. Int. Ed*., 2010, **49**, 3939.

33 F. J. M. Hoeben, P. Jonkheijm, E. W. Meijer and A. P. H. J. Schenning, *Chem. Rev*., 2005, **105**, 1491.

34 E. M. Kosower, J. L. Cotter, *J. Am. Chem. Soc*., 1964, **86**, 5524.

35 W. S. Jeon, H.-J. Kim, C. Lee and K. Kim, *Chem. Commun*., 2002, 1828.

36 Y. H. Ko, E. Kim, I. Hwang and K. Kim, *Chem. Commun*., 2007, 1305; Y. H. Ko, I. Hwang, D.-W. Lee and K. Kim, *Israel J. Chem*., 2011, **51**, 506.

37 H. Li, A. C. Fahrenbach, S. K. Dey, S. Basu, A. Trabolsi, Z. Zhu, Y. Y. Botros and J. F. Stoddart, *Angew. Chem. Int. Ed*., 2010, **49**, 8260; A. Trabolsi, N. Khasha, A. C. Fahrenbach, D. C. Friedman, M. T. Colvin, K. K. Cotí, D. Benítez, E. Tkatchouk, J.-C. Olsen, M. E. Belowich, R. Carmielli, H. A. Khatib, W. A. Goddard, M. P. Wasielewski and J. F. Stoddart, *Nature Chem*., 2010, **2**, 42.

38 A. Iordache, M. Oltean, A. Milet, F. Thomas, B. Baptiste, E. Saint-Aman and C. Bucher, *J. Am. Chem. Soc*., 2012, **134,** 2653.

39 J. C. Evans, A. G. Evans, N. H. Nouri-Sorkhabi, A. Y. Obaid and C. C. Rowlands, *J. Chem. Soc. Perkin Trans. 2*, 1985, 315.

40 J. C. Barnes, A. C. Fahrenbach, S. M. Dyar, M. Frasconi, M. A. Giesener, Z. Zhu, Z. Liu, K. J. Hartlieb, R. Carmieli, M. R. Wasielewski and J. F. Stoddart, *Proc. Natl. Acad. Sci. U.S.A.*, 2012, **109**, 11546.

TOC

Without or with the assistance of CB[8], a triangular radical monomer can self-assemble into 2D supramolecular organic frameworks in water.